

Circumstellar structures around high-mass X-ray binaries

Vasilii V. Gvaramadze^{1,2}

¹Sternberg Astronomical Institute, Lomonosov Moscow State University, Universitetskij Pr. 13, Moscow 119992, Russia
email: vgvaram@mx.iki.rssi.ru

²Space Research Institute, Russian Academy of Sciences, Profsoyuznaya 84/32, 117997 Moscow, Russia

Abstract. Many high-mass X-ray binaries (HMXBs) are runaways. Stellar wind and radiation of donor stars in HMXBs along with outflows and jets from accretors interact with the local interstellar medium and produce curious circumstellar structures. Several such structures are presented and discussed in this contribution.

Keywords. Circumstellar matter, stars: individual (4U 1907+09, EXO 1722-363, HD 34921, GX 304-01, Vela X-1, IGR J16327–4940), ISM: bubbles, X-rays: binaries.

1. Introduction

The high space velocities of HMXBs could be revealed via measurement of proper motions and/or radial velocities of these systems, or through the detection of bow shocks – the secondary attributes of runaway systems. The first detection of a bow shock produced by a HMXB was reported by Kaper *et al.* (1997), who discovered an H α arc around Vela X-1. Later, Huthoff & Kaper (2002) searched for bow shocks around eleven high-velocity HMXBs using *IRAS* maps, but did not find new ones.

Our search for bow shocks around HMXBs from the sample of Huthoff & Kaper (2002) using data from the *Spitzer Space Telescope* led to the discovery of a bow shock associated with 4U 1907+09 (Fig. 1; cf. Gvaramadze *et al.* 2011). An asymmetric shape of the bow shock could be caused by density inhomogeneities in the local interstellar medium (ISM), as evidenced by the *Herschel* images of the field around 4U 1907+09 (see Fig. 1). The runaway nature of this HMXB is supported by proper motion measurements. Particularly,

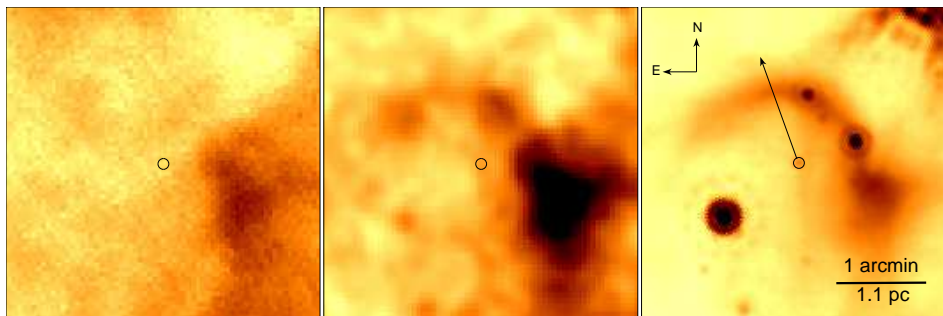


Figure 1. From left to right: *Herschel* 160 and 70 μm , and *Spitzer* 24 μm images of the field containing 4U 1907+09 (indicated by a circle). The arrow shows the direction of motion of 4U 1907+09, as follows from the *Gaia* proper motion measurement.

the *Gaia* DR2 (Gaia Collaboration 2018) proper motion and distance (≈ 4 kpc; Bailer-Jones *et al.* 2018) of 4U 1907+09 indicate that this system has a peculiar (transverse) velocity of $\approx 200 \text{ km s}^{-1}$, which is the highest peculiar velocity measured for HMXBs.

2. EXO 1722-363, HD 34921 & GX 304-01

We also searched for bow shocks around other HMXBs covered by *Spitzer* but, surprisingly, did not find any. Instead, we detected curious infrared nebulae around several HMXBs, two of which are presented below (both were independently discovered by Prišegen 2018). Fig. 2 shows a tau-shaped nebula associated with EXO 1722-363. The shape of the nebula and position of EXO 1722-363 within it exclude the bow shock interpretation for this nebula. Although one cannot exclude the possibility that the nebula is produced by collimated outflows (jets) from this HMXB (cf. Gallo *et al.* 2005; Heinz *et al.* 2008), the more plausible explanation is that we deal with a local ISM heated by radiation from the B0–1 Ia (Mason *et al.* 2009) companion star in EXO 1722-363.

Fig. 3 shows the *Spitzer* $24 \mu\text{m}$ image of a barrel-like nebula around HD 34921 in two intensity scales to highlight some details of its filamentary structure. From the *Gaia* data and the heliocentric radial velocity of HD 34921 of -20.5 km s^{-1} (Gontcharov 2008), we derive the peculiar velocity of this star of $\approx 30 \text{ km s}^{-1}$. Although this velocity is typical of runaway stars, the complex shape of the nebula excludes its interpretation as a pure bow shock.

With the advent of the *Wide-field Infrared Survey Explorer* (*WISE*), it became possible to search for bow shocks around all (~ 100 ; e.g. Liu *et al.* 2006) known HMXBs,

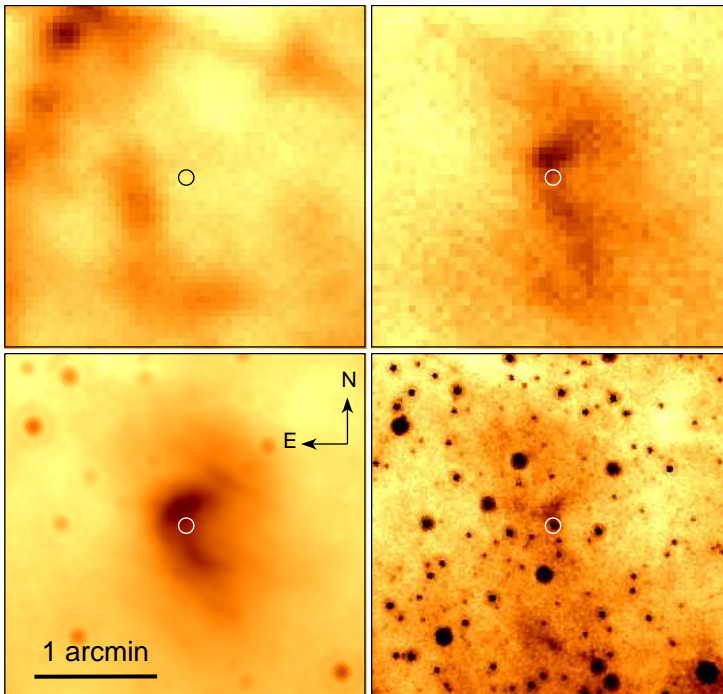


Figure 2. From left to right and from top to bottom: *Herschel* 160 and $70 \mu\text{m}$, and *Spitzer* 24 and $8 \mu\text{m}$ images of the field containing EXO 1722-363 (indicated by a circle).

and what is absolutely amazing is that we did not find new bow shocks at all! The only interesting discovery is a bow-like structure attached to GX 304-1 (independently detected by Prišegen 2018). The geometry of this structure (see Fig. 4) and the weak wind of the B2 Vne (Parkes *et al.* 1980) donor star in GX 304-1 suggest that here we deal with a radiation-pressure-driven bow wave (cf. van Buren & McCray 1988; Ochsendorf *et al.* 2014), although other explanations (involving jets or illumination of the local ISM) cannot be excluded as well.

3. Vela X-1

We also discovered a filamentary structure stretched behind the high-velocity ($\approx 50 \text{ km s}^{-1}$) HMXB Vela X-1. Fig. 5 shows the SuperCOSMOS H-alpha Survey (SHS; Parker *et al.* 2005) $H\alpha$ image of this structure along with the already known bow shock ahead of Vela X-1. The geometry of the filaments suggests that Vela X-1 has met a wedge-like layer of enhanced density on its way and that the shocked material of this layer outlines a wake downstream of Vela X-1.

To substantiate this suggestion, we carried out 3D MHD simulations of interaction between Vela X-1 and the layer for three limiting cases (see Fig. 6): the stellar wind and the ISM were treated as pure hydrodynamic flows (model 1); a homogeneous magnetic field was added to the ISM, while the stellar wind was assumed to be unmagnetized (model 2); the stellar wind was assumed to possess a helical magnetic field (described by the Parker solution; Parker 1958), while there was no magnetic field in the ISM (model 3). We found that although the first two models can provide a rough agreement with the observations (cf. Fig. 7 with Fig. 5), only the third one allowed us to reproduce not only the wake behind Vela X-1, but also the opening angle of the bow shock and the apparent detachment of its eastern wing from the wake (for more details see Gvaramadze *et al.* 2018a).

4. IGR J16327–4940

Masetti *et al.* (2010) detected an OB star within the error circle of the *INTEGRAL* transient source of hard X-ray emission IGR J16327–4940 (Bird *et al.* 2010) and classified

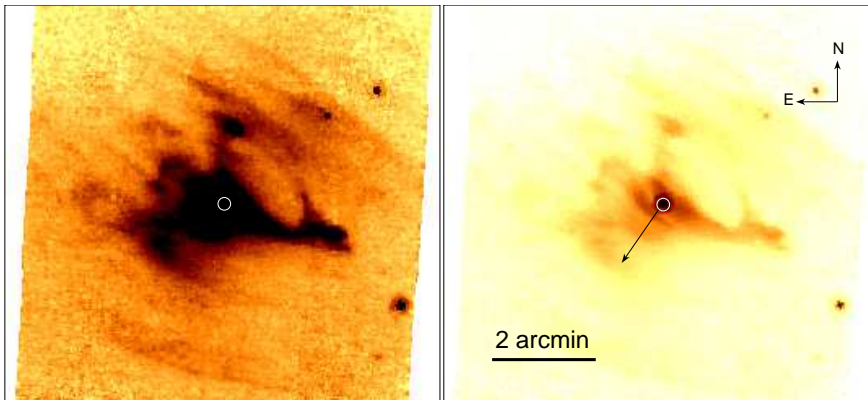


Figure 3. *Spitzer* 24 μm image of the barrel-like nebula around HD 34921 (indicated by a circle) in two intensity scales. The arrow shows the direction of motion of HD 34921.

this source as a HMXB because of its ‘overall early-type star spectral appearance, which is typical of this class of objects’.

Using *Spitzer* data, we found that the optical counterpart to IGR J16327–4940 is surrounded by a circular nebula (see Fig. 8), named MN44 in Gvaramadze *et al.* (2010). A spectrum of the central star of MN44 taken in 2009 shows hydrogen and iron lines in emission, which is typical of luminous blue variables (LBVs) near the visual maximum (Gvaramadze *et al.* 2015). New observations carried out in 2015 revealed significant changes in the spectrum, indicating that the star became hotter. The spectral variability was accompanied by ≈ 1.6 mag changes in the brightness, meaning that IGR J16327–4940 is a bona fide LBV (Gvaramadze *et al.* 2015).

Gaia DR2 data indicate that IGR J16327–4940 is a high-velocity ($\approx 75 \text{ km s}^{-1}$) runaway system ejected $\approx 4 - 5$ Myr ago from one of the most massive star clusters in the Milky Way — Westerlund 1 (Gvaramadze 2018), while a perfectly circular shape of the associated nebula implies that it does not feel the effect of ram pressure of the ISM. This means that the stellar wind still interacts with a co-moving dense material lost by the star during the preceding (e.g. red supergiant) evolutionary stage (cf. Gvaramadze *et al.* 2009) or because of binary interaction processes (if this star is or was a binary system; cf. Gvaramadze *et al.* 2018b). If the HMXB nature of IGR J16327–4940 will be confirmed, then this system would represent a first known example of an HMXB with an LBV donor star.

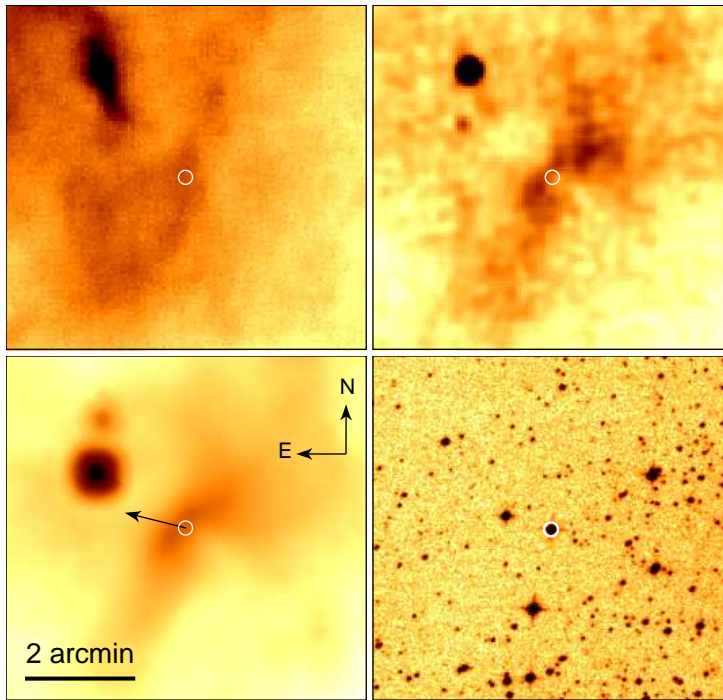


Figure 4. From left to right and from top to bottom: *Herschel* 160 and 70 μm , *WISE* 22 μm and DSS-II red-band images of the field containing GX 304-01 (indicated by a circle). The arrow shows the direction of motion of GX 304-01.

5. Conclusions

A possible explanation of the non-detection of bow shocks around HMXBs is that most of these systems are moving through a low-density, hot medium, so that the emission measure of their bow shocks is below the detection limit or the bow shocks do not form at all because the sound speed in the local ISM is higher than the stellar peculiar velocity (Huthoff & Kaper 2002). This provides a reasonable explanation of why only one-fifth of runaway OB stars produce (observable) bow shocks (van Buren *et al.* 1995). The detection rate of bow shocks around HMXBs is, however, a factor of ten less than that for OB stars (cf. Prišegen 2018). This difference could be understood if the HMXBs have systematically lower space velocities compared to the ordinary runaway stars (ejected in the field mostly because of dynamical few-body interactions), which could be connected to the formation mechanism of HMXBs (e.g. the supernova explosions in the HMXB progenitors should not be too energetic to unbind them). Moreover, the large proportion of HMXBs with (weak-wind) Be donor stars (Coleiro *et al.* 2013) could also contribute to this difference.

This work was supported by the Russian Science Foundation grant No. 14-12-01096.

References

- Bailer-Jones, C.A.L., Rybizki J., Fouesneau, M., Mantelet, G., & Andrae, R. 2018, *AJ*, 156, 58
 Bird A.J., *et al.* 2010, *ApJS*, 186, 1
 Coleiro, A., Chaty, S., Zurita Heras, J.A., Rahoui, F., & Tomsick, J.A. 2013, *A&A*, 560, A108
 Gaia Collaboration Brown, A.G.A., Vallenari, A., Prusti, T., de Bruijne, J.H.J., Babusiaux, C., & Bailer-Jones, C.A.L. 2018, *A&A*, 616, A1
 Gallo, E., Fender, R., Kaiser, C., Russell, D., Morganti, R., Oosterloo, T., & Heinz S. 2005, *Nature*, 436, 819
 Gontcharov, G.A. 2006, *Astron. Lett.*, 32, 759
 Gvaramadze, V. V. 2018, *RNAAS*, in press; preprint arXiv:1811.07899

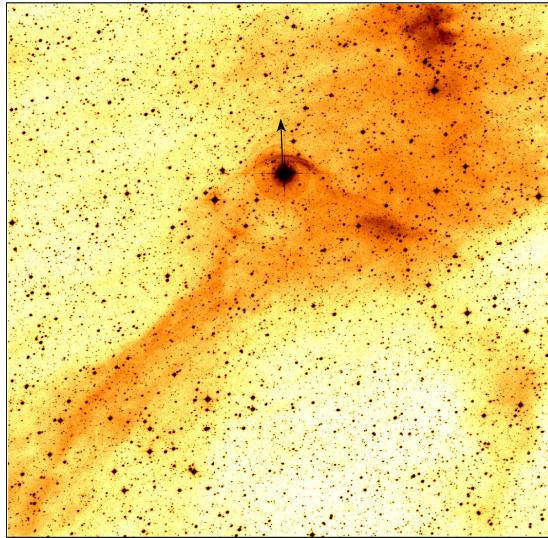


Figure 5. SHS H α image of a 30 arcmin \times 30 arcmin field containing Vela X-1 and filamentary structures behind it. The arrow shows the direction of motion of Vela X-1.

- Gvaramadze, V. V., *et al.* 2009, *MNRAS*, 400, 524
 Gvaramadze, V. V., Kniazev, A. Y., & Fabrika, S. 2010, *MNRAS*, 405, 1047
 Gvaramadze, V. V., Röser, S., Scholz, R.-D., & Schilbach, E. 2011, *A&A*, 529, A14
 Gvaramadze, V. V., Kniazev, A. Y., & Berdnikov, L. N. 2015, *MNRAS*, 454, 3710
 Gvaramadze, V. V., Alexashov, D. B., Katushkina, O. A., & Kniazev, A. Y. 2018a, *MNRAS*, 474, 4421
 Gvaramadze, V. V., Maryeva, O. V., Kniazev, A. Y., Alexashov, D. B., Castro, N., Langer, N., & Katkov, I. Y. 2018b, *MNRAS*, in press; arXiv:1810.12916
 Heinz, S., Grimm, H.J., Sunyaev, R.A., & Fender, R.P. 2008, *ApJ*, 686, 1145
 Huthoff, F., & Kaper, L. 2002, *A&A*, 383, 999
 Kaper, L., van Loon, J. Th., Augusteijn, T., Goudfrooij, P., Patat, F., Waters, L. B. F. M., & Zijlstra, A. A. 1997, *ApJ* (Letters), 5475, L37
 Liu, Q.Z., van Paradijs, J., & van den Heuvel, E.P.J. 2006, *A&A*, 455, 1165
 Masetti, N., *et al.* 2010, *A&A*, 519, A96
 Mason, A.B., Clark, J.S., Norton, A.J., Negueruela, I., & Roche, P. 2009, *A&A*, 505, 281
 Ochsendorf, B.B., *et al.* 2014, *A&A*, 563, A65
 Parker, E.N. 1958, *ApJ*, 128, 664
 Parker, Q., *et al.* 2005, *MNRAS*, 362, 689
 Parkes, G.E., Murdin, P.G., & Mason, K.O. 1980, *MNRAS*, 190, 537
 Prišegen, M. 2018, *A&A*, in press; arXiv:1811.06781
 van Buren, D., & McCray, R. 1988, *ApJ*, 329, L93
 van Buren, D., Noriega-Crespo, A., & Dgani, R. 1995, *AJ*, 110, 2914

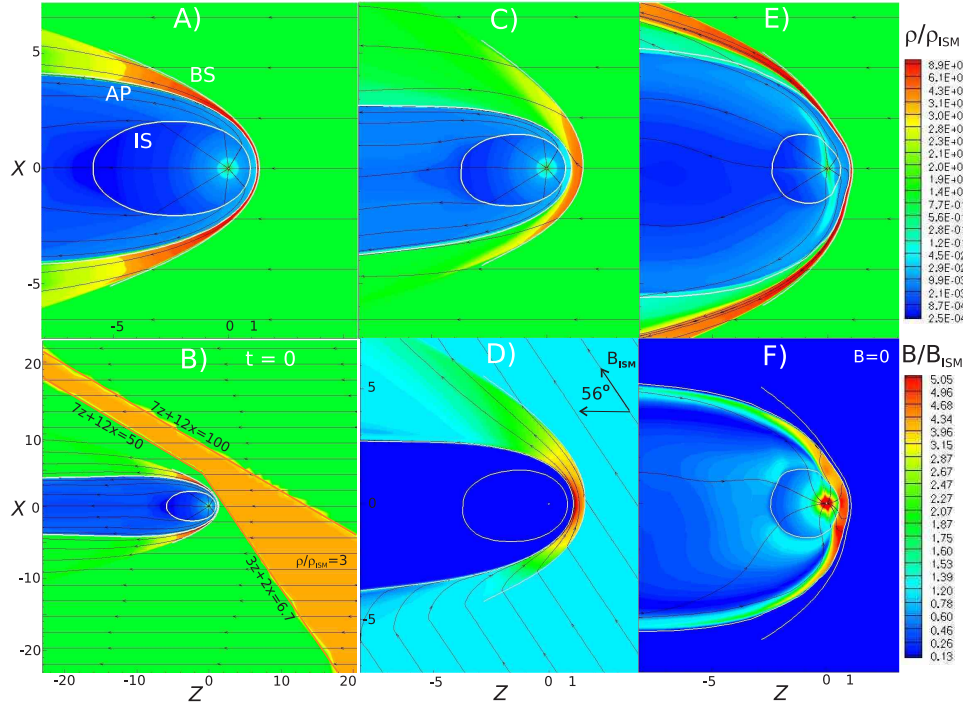


Figure 6. 2D distributions of the plasma density and streamlines (panels A, C, and E) and the magnetic field with the field lines (panels D and F) in the steady-state models. Panel A corresponds to model 1, panels C and D to model 2, and panels E and F to model 3. Panel B shows the initial condition in the ISM for the non-stationary models (shown in Fig. 7). The inner shock (IS), the astropause (AP) and the bow shock (BS) are plotted with white lines. Adopted from Gvaramadze *et al.* (2018a).

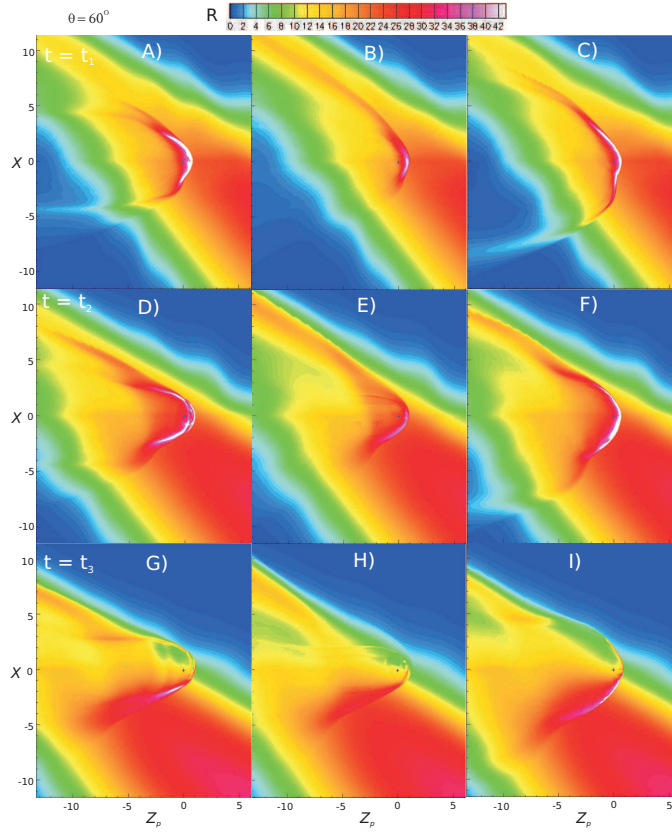


Figure 7. Projection of synthetic H α intensity maps with a line of sight at an angle of $\theta = 60^\circ$ to the symmetry axes of the non-stationary models 1, 2, and 3 (left to right) at three times (top to bottom). Adopted from Gvaramadze *et al.* (2018a).

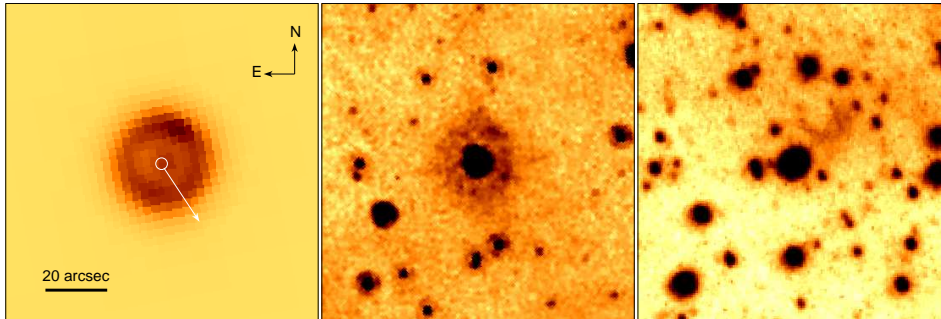


Figure 8. From left to right: *Spitzer* 24 and $8\mu\text{m}$, and SHS H α images of the field containing IGR J16327–4940 (indicated by a circle) and its circumstellar nebula. The arrow shows the direction of motion of IGR J16327–4940.